

Hydrogen Storage in High Surface Area Carbons: Experimental Demonstration of the Effects of Nitrogen Doping

Yongde Xia,[†] Gavin S. Walker,[†] David M. Grant,[†] and Robert Mokaya*[‡]

*Division of Fuels and Power Technology, Faculty of Engineering, and School of Chemistry,
University of Nottingham, University Park, Nottingham NG7 2RD, United Kingdom*

Received July 3, 2009; E-mail: r.mokaya@nottingham.ac.uk

Abstract: The influence of nitrogen doping on the hydrogen uptake and storage capacity of high surface area carbon materials is presented in this report. To generate suitable study materials, we have exploited the relationship between synthesis conditions and textural properties of zeolite-templated carbons to generate a range of high surface area carbons with similar pore size distribution but which are either N-doped or N-free. For N-doped carbons, the nitrogen content was kept within a narrow range of between 4.7 and 7.7 wt %. The carbon materials, irrespective of whether they were doped or not, exhibited high surface area (1900–3700 m²/g) and pore volume (0.99 and 1.88 cm³/g), a micropore surface area of 1500–2800 m²/g, and a micropore volume of 0.65–1.24 cm³/g. The hydrogen uptake varied between 4.1 and 6.9 wt %. We present experimental data that indicates that the effect of N-doping on hydrogen uptake is only apparent when related to the surface area and pore volume associated with micropores rather than total porosity. Furthermore, by considering the isosteric heat of hydrogen adsorption and excess hydrogen uptake on N-free or N-doped carbons, it is shown that N-doping can be beneficial at lower coverage (low hydrogen uptake) but is detrimental at higher coverage (higher hydrogen uptake). The findings are consistent with previous theoretical predictions on the effect of N-doping of carbon on hydrogen uptake. The findings, therefore, add new insights that are useful for the development of carbon materials with enhanced hydrogen storage capacity.

Introduction

Porous carbons that have high surface area and well-ordered pore systems are potentially useful as hydrogen storage materials.¹ Highly porous carbons may be prepared via a variety of methods including activation (physical or chemical)² or template carbonization.^{3,4} The template carbonization method, which involves the introduction of suitable carbon precursors into the pores of a hard (inorganic) template followed by carbonization and finally removal of the template, is attractive for the formation of carbons with controlled porosity.^{3,4} Several factors, including textural parameters^{5–11} and surface properties,¹² are known to determine the hydrogen storage capacity of porous carbons. To date, studies suggest that the most important factors in determining hydrogen uptake are surface area, pore volume, and pore size. A number of studies have reported on the link between surface area (associated with microporosity) and hydrogen storage^{5–11} and, furthermore, have suggested that micropores below 10 Å,⁹ and preferably 6–8 Å,^{5,6,8–11} are the

most efficient for hydrogen uptake. On the other hand, there are hardly any *experimental* studies on the effect of the carbon surface properties (i.e., functionality) and, in particular, the presence of heteroatoms *within* the carbon network on hydrogen storage.¹³ This is despite several theoretical studies that predict changes in hydrogen uptake of porous carbons due to heteroatom substitution of carbon.^{14–16} Of interest is nitrogen-doping, which

[†] Division of Fuels and Power Technology.

[‡] School of Chemistry.

- (1) (a) van den Berg, A. W. C.; Arean, C. O. *Chem. Commun.* **2008**, 668. (b) Ströbel, R.; Garcke, J.; Moseley, P. T.; Jörisen, L.; Wolf, G. *J. Power Sources* **2006**, 159, 781. (c) Thomas, K. M. *Catal. Today* **2007**, 120, 389.
- (2) Ahmadpour, A.; Do, D. D. *Carbon* **1996**, 34, 471.
- (3) (a) Ryoo, R.; Joo, S. H.; Kruk, M.; Jaroniec, M. *Adv. Mater.* **2001**, 13, 677. (b) Yang, H. F.; Zhao, D. Y. *J. Mater. Chem.* **2005**, 15, 1217. (c) Lee, J.; Han, S.; Hyeon, T. *J. Mater. Chem.* **2004**, 14, 478. (d) Lee, J.; Kim, J.; Hyeon, T. *Adv. Mater.* **2006**, 18, 2073.
- (4) Kyotani, T. *Bull. Chem. Soc. Jpn.* **2006**, 79, 1322.

- (5) Texier-Mandoki, N.; Dentzer, J.; Piquero, T.; Saadallah, S.; David, P.; Vix-Guterl, C. *Carbon* **2004**, 42, 2744.
- (6) Rzepka, M.; Lamp, P.; De la Casa-Lillo, M. A. *J. Phys. Chem. B* **1998**, 102, 10894.
- (7) (a) Armandi, M.; Bonelli, B.; Arean, C. O.; Garrone, E. *Microporous Mesoporous Mater.* **2008**, 112, 411. (b) Xu, W. C.; Takahashi, K.; Matsuo, Y.; Hattori, Y.; Kumagai, M.; Ishiyama, S.; Kaneko, K.; Iijima, S. *Int. J. Hydrogen Energy* **2007**, 32, 2504.
- (8) de la Casa-Lillo, M. A.; Lamari-Darkrim, F.; Cazorla-Amoros, D.; Linares-Solano, A. *J. Phys. Chem. B* **2002**, 106, 10930.
- (9) (a) Gogotsi, Y.; Dash, R. K.; Yushin, G.; Yildirim, T.; Laudisio, G.; Fischer, J. E. *J. Am. Chem. Soc.* **2005**, 127, 16006. (b) Vix-Guterl, C.; Frackowiak, E.; Jurewicz, K.; Friebel, M.; Parmentier, J.; Beguin, F. *Carbon* **2005**, 43, 1293. (c) Yushin, G.; Dash, R.; Jagiello, J.; Fischer, J. E.; Gogotsi, Y. *Adv. Funct. Mater.* **2006**, 16, 2288.
- (10) Cabria, I.; Lopez, M. J.; Alonso, J. A. *Carbon* **2007**, 45, 2649.
- (11) Yang, Z.; Xia, Y.; Mokaya, R. *J. Am. Chem. Soc.* **2007**, 129, 1673.
- (12) Benard, P.; Chahine, R. *Scr. Mater.* **2007**, 56, 803.
- (13) (a) Zhao, X. B.; Xiao, B.; Fletcher, A. J.; Thomas, K. M. *J. Phys. Chem. B* **2005**, 109, 8880. (b) Badzian, A.; Badzian, T.; Brevail, E.; Piotrowski, A. *Thin Solid Films* **2001**, 398, 170.
- (14) (a) Sankaran, M.; Viswanathan, B. *Carbon* **2006**, 44, 2816. (b) Sankaran, M.; Viswanathan, B.; Murthy, S. S. *Int. J. Hydrogen Energy* **2008**, 33, 393.
- (15) Zhou, Z.; Gao, X.; Yan, J.; Song, D. *Carbon* **2006**, 44, 939.
- (16) Zhu, Z. H.; Hatori, H.; Wang, S. B.; Lu, G. Q. *J. Phys. Chem. B* **2005**, 109, 16744.

is predicted to cause changes in hydrogen uptake of carbons.^{15,16} It is therefore of interest to experimentally probe the effect of nitrogen doping on the hydrogen storage capacity of high surface area carbons.

Any proper investigation of the effects of heteroatom (nitrogen) substitution must, however, ensure that the other key properties of the carbons remain unchanged. A key variable that should be kept constant or within a very limited range is pore size.^{5–11} Recent studies have shown that the pore size of porous carbons prepared via template carbonization using zeolites as templates can be controlled within a narrow range.^{11,17–20} The basis of controlling the pore size in the resulting zeolite-templated carbons is replication of the structural regularity of zeolite templates in the carbons.^{11,17–20} Zeolite-templating can therefore generate a suite of carbons with similar pore size but with varied surface functionality, thus enabling an experimental investigation of the effects of the later on hydrogen storage. In this study, we have exploited the relationship between synthesis conditions and pore size of zeolite-templated carbons to generate a range of high surface area carbons with similar pore size distribution but that are either N-doped or N-free, in an attempt to demonstrate the effect of N-doping on hydrogen storage capacity. We find that an effect of N-doping on hydrogen uptake can be observed when uptake is related to the surface area and pore volume associated with micropores. Our findings provide further evidence that pores larger than an optimum micropore size have a lesser contribution to hydrogen storage in carbon materials.

Experimental Section

Material Synthesis. To obtain carbon materials, zeolite EMC-2, Y, or 13X were used as templates, and furfuryl alcohol (FA), acetonitrile (AN), and ethylene (ET) were used as carbon precursors. Acetonitrile-derived carbons were prepared as follows: 0.6 g of zeolite (EMC-2 or Y) in an alumina boat was placed in a flow through tube furnace. The furnace was heated to a target temperature between 750 and 900 °C under a flow of argon and then maintained at the target temperature for 3 h under a flow of argon saturated with acetonitrile to allow chemical vapor deposition (CVD) of carbon into the zeolite. The gas flow was switched to argon only and the temperature of the furnace was raised to (or kept at) 900 °C and maintained for 3 h in a flow of argon only, followed by cooling down to room temperature under argon. The resulting zeolite/carbon composites were washed with 10% hydrofluoric (HF) acid several times and then refluxed at 60 °C in concentrated hydrochloric acid (HCl) to remove the zeolite framework and finally oven-dried at 120 °C. Carbons nanocast from zeolite EMC-2 were designated as CMXAN, where X is the CVD temperature (750, 800, 850, or 900 °C), and one sample derived from zeolite Y was designated as CY800AN. Two ethylene-derived samples were prepared from zeolite Y and 13X as follows: 0.6 g of zeolite (Y or 13X) was exposed to a flow of ethylene at 700 °C for 3 h, followed by heat treatment at 900 °C in a flow of argon only for 3 h. Removal

of zeolite template was as described above generating sample CY700ET and CX700ET from zeolite Y and 13X, respectively.

Three samples were prepared using a combination of liquid impregnation (LI) and CVD as follows:¹⁹ 0.6 g of zeolite (EMC-2, Y, or 13X), previously dried in the oven at 300 °C, was impregnated with furfuryl alcohol, which was polymerized under argon at 80 °C for 24 h and then at 150 °C for 8 h, followed by pyrolysis at 700 °C under argon for 3 h. The resulting carbon/zeolite composite was then placed in a flow through furnace and exposed to CVD with ethylene gas at 700 °C for 3 h. The gas flow was switched to argon only and the temperature of the furnace raised to 900 °C and maintained for 3 h in a flow of argon only, followed by cooling to room temperature under argon. The carbon/zeolite composite was washed with HF and HCl then dried as described above generating carbons designated as CMFAET, CYFAET, and CXFAET from zeolite EMC-2, Y, and 13X respectively.

Material Characterization. Powder XRD analysis was performed using a Philips 1830 powder diffractometer with Cu K α radiation (40 kV, 40 mA). Nitrogen sorption isotherms and textural properties of the carbons were determined at –196 °C using nitrogen in a conventional volumetric technique by an Autosorb-1 sorptometer. Before analysis, the samples were evacuated for 12 h at 300 °C under vacuum. The surface area was calculated using the BET method based on adsorption data in the partial pressure (P/P_0) range 0.02–0.22 and total pore volume was determined from the amount of the nitrogen adsorbed at $P/P_0 \approx 0.99$. Micropore surface area and micropore volume were obtained via t -plot analysis. Elemental analysis was carried out using a CHNS analyzer (Fisons EA 1108). Thermogravimetric analysis (TGA) was performed using a Perkin-Elmer TGA 6 analyzer with a heating rate of 2 °C/min under static air conditions. X-ray photoelectron spectroscopy (XPS) was performed using a Kratos AXIS ULTRA spectrometer with a monochromated Al K α X-ray source (1486.6 eV) operated at 10 mA emission current and 15 kV anode potential. The analysis chamber pressure was better than 1.3×10^{-12} bar. The take off angle for the photoelectron analyzer was 90° and the acceptance angle was 30° (in magnetic lens modes).

Hydrogen Uptake Measurements. The excess hydrogen uptake capacity of the carbons was measured by gravimetric analysis with an Intelligent Gravimetric Analyzer, IGA (Hiden), using 99.9999% purity hydrogen additionally purified by a molecular sieve filter. The hydrogen uptake measurements were performed at –196 °C (in a liquid nitrogen bath) over the pressure range 0–20 bar. The samples were outgassed (10^{-10} bar) under heating at 200 °C overnight before measurement. The hydrogen uptake data was rigorously corrected for the buoyancy of the system and samples. The excess hydrogen uptake was calculated on the basis of a density of 1.5 g/cm³ for the carbon samples. The carbon density (1.5 g/cm³) used in the buoyancy corrections was determined from helium sorption data obtained using the IGA at a pressure of up to 20 bar at 273 K. The total hydrogen uptake was calculated from the measured excess capacity by taking into account the pore volume of the samples and the density of compressed hydrogen at the prevailing temperature and pressure.²¹ In all cases, the hydrogen uptake (excess or total) is reported as wt% of carbon sample weight. The isosteric heat of adsorption (Q_{st}) was calculated using hydrogen uptake isotherms measured at two different temperatures (–196 °C (liquid nitrogen) and –186 °C (liquid argon)) based on the Clausius–Clapeyron equation. We also obtained volumetric hydrogen sorption data (performed at General Motors, Warren, MI) using Sievert's apparatus (PCT-Pro 2000) with high purity hydro-

- (17) (a) Kyotani, T. *Carbon* **2000**, *38*, 269. (b) Kyotani, T.; Ma, Z. X.; Tomita, A. *Carbon* **2003**, *41*, 1451. (c) Ma, Z.; Kyotani, T.; Liu, Z.; Terasaki, O.; Tomita, A. *Chem. Mater.* **2001**, *13*, 4413. (d) Ma, Z. X.; Kyotani, T.; Tomita, A. *Chem. Commun.* **2000**, 2365. (e) Hou, P.-X.; Oriksa, H.; Yamazaki, T.; Matsuoka, K.; Tomita, A.; Setoyama, N.; Fukushima, Y.; Kyotani, T. *Chem. Mater.* **2005**, *17*, 5187.
- (18) (a) Garsuch, A.; Klepel, O.; Sattler, R. R.; Berger, C.; Glaeser, R.; Weitkamp, J. *Carbon* **2006**, *44*, 593. (b) Garsuch, A.; Klepel, O. *Carbon* **2005**, *43*, 2330.
- (19) Gaslain, F. O. M.; Parmentier, J.; Valtchev, V. P.; Patarin, J. *Chem. Commun.* **2006**, 991.
- (20) (a) Yang, Z.; Xia, Y.; Sun, X.; Mokaya, R. *J. Phys. Chem. B* **2006**, *110*, 18424. (b) Pacula, A.; Mokaya, R. *J. Phys. Chem. C* **2008**, *112*, 2764.

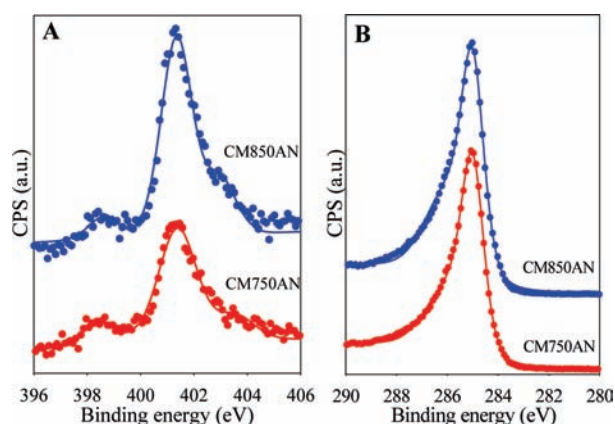
- (21) Yan, Y.; Lin, X.; Yang, S. H.; Blake, A. J.; Dailly, A.; Champness, N. R.; Hubberstey, P.; Schroder, M. *Chem. Commun.* **2009**, 1025.

- (22) (a) Casanovas, J.; Ricart, J. M.; Rubio, J.; Illas, F.; Jimenez-Mateos, J. M. *J. Am. Chem. Soc.* **1996**, *118*, 8071. (b) Sen, R.; Satishkumar, B. C.; Govindaraj, A.; Harikumar, K. R.; Renganathan, M. K.; Rao, C. N. R. *J. Mater. Chem.* **1997**, *7*, 2335. (c) Terrones, M.; Redlich, P.; Grobert, N.; Trasobares, S.; Hsu, W.-K.; Terrones, H.; Zhu, Y.-Q.; Hare, J. P.; Reeves, C. L.; Cheetham, A. K.; Rühle, M.; Kroto, H. W.; Walton, D. R. M. *Adv. Mater.* **1999**, *11*, 655.

Table 1. Textural Properties, Nitrogen Content, and Hydrogen Uptake of Zeolite-Templated Carbons (see Experimental Section for Sample Designation)

sample	N content ^a (wt %)	surface area ^b (m ² /g)	pore volume ^c (cm ³ /g)	H ₂ uptake ^{d,e} (wt %)
CM750AN	4.7 (5.2)	3360 (2838)	1.71 (1.24)	6.4 (5.3)
CM800AN	6.5 (7.6)	2762 (2302)	1.41 (0.99)	5.7 (4.8)
CM850AN	6.3 (6.5)	2658 (2167)	1.42 (0.98)	5.4 (4.5)
CM900AN	6.2 (5.9)	2168 (1761)	1.11 (0.75)	4.5 (3.8)
CMFAET	0	3698 (2821)	1.88 (1.14)	6.9 (5.7)
CY700ET	0	2017 (1571)	1.10 (0.66)	4.7 (4.0)
CYFAET	0	1972 (1510)	1.17 (0.65)	4.5 (3.8)
CY800AN	7.7	1912 (1528)	0.99 (0.65)	4.1 (3.4)
CX700ET	0	2466 (1686)	1.41 (0.69)	5.1 (4.2)
CXFAET	0	2841 (2242)	1.54 (0.95)	6.3 (5.3)

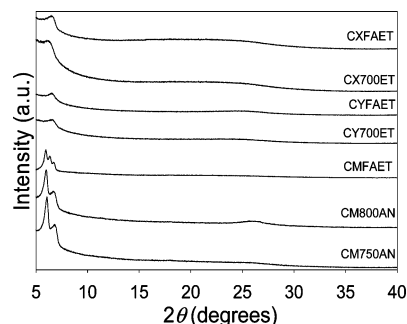
^a Values in parentheses are obtained from XPS analysis. ^b Values in parentheses are micropore surface area. ^c Values in parentheses are micropore volume. ^d Total hydrogen uptake capacity at -196 °C and 20 bar. ^e Values in parentheses are excess hydrogen adsorption at -196 °C and 20 bar.

**Figure 1.** N 1s (A) and C 1s (B) peaks in the XPS spectra of N-doped zeolite-templated carbons.

gen.²¹ The volumetric measurements allowed an independent verification of the IGA hydrogen uptake measurements.

Results and Discussion

For all carbon samples in this study, thermogravimetric analysis indicated a residual mass, at 800 °C, typically lower than 1%, confirming that the carbons were virtually zeolite-free. The nitrogen content of the carbon samples, given as wt%, is shown in Table 1. Two sets of carbons are generated: N-doped and N-free. The nitrogen content determined via bulk elemental analysis varies between 4.7 and 7.7 wt % for samples derived from acetonitrile. We have previously shown that the use of acetonitrile as single precursor ensures that the nitrogen is homogeneously distributed in these N-doped carbon materials.²⁰ This is confirmed by the fact that the nitrogen content determined from X-ray photoelectron spectroscopy (XPS) analysis (a surface technique) is in all cases very close to the bulk elemental analysis values (Table 1). The N is, therefore, as expected, uniformly distributed throughout the samples in both the external and internal surfaces and within the bulk. The “surface” N content (determined by XPS) is, however of particular importance, as it gives a direct indication of the amount of N present on the carbon surface that interacts with and adsorbs hydrogen. XPS analysis also provided information on the nature of the binding between carbon and nitrogen. Similar to previous results, the XPS spectra (Figure 1) exhibited a N 1s signal split into two main peaks; an intense peak at 401.2

**Figure 2.** Powder XRD patterns of zeolite-templated carbons.

eV and a lower intensity peak at about 398.5 eV along with a shoulder peak at about 403.2 eV.^{20,22} The spectra indicate that the N-doped carbons possess highly coordinated (quaternary) “pyrrolic” nitrogen atoms (401.2 eV) incorporated into graphene sheets, along with pyridine-like nitrogen atoms incorporated into graphene sheets (398.5 eV).^{20,22} The peak at 403.2 eV is slightly higher than that expected for inner “graphitic” N atoms^{23a} and may, therefore, arise from graphitic N atoms that are coordinated to O atoms.^{20,22} The O atoms may arise from the replication process which involves contact with various oxygen containing reagents (zeolite template and aqueous acid). The C 1s peak for the N-doped carbon materials was observed at about 284.9 eV, consistent with graphene sp² carbon.

Figure 2 shows powder X-ray diffraction (XRD) patterns of the carbon materials. For samples derived from zeolite EMC-2 (CM750AN, CM800AN and CMFAET), the XRD patterns show a peak, similar to the (100) diffraction of the zeolite EMC-2 template, at $2\theta = 6.1^\circ$. This peak indicates that these carbons exhibit structural pore ordering similar to that of the zeolite.^{8,10–13} The patterns show a further peak at $2\theta = 6.8^\circ$, which is at a position similar to the (002), (101) diffractions of zeolite EMC-2, confirming the replication of zeolite-type structural ordering in the carbons (the XRD patterns of samples CM850AN and CM900AN are similar to that of sample CM800AN). The XRD patterns of samples derived from zeolite Y (CY700ET and CYFAET) show a peak at $2\theta = 6^\circ$ that is similar to the (111) peak of zeolite Y. The XRD patterns of samples derived from zeolite 13X (CX700ET and CXFAET) also show a peak, similar to that of zeolite 13X, at about $2\theta = 6^\circ$. The XRD patterns in Figure 2 therefore confirm that the carbons are well ordered and zeolite-like, with comparable levels of zeolite-type structural ordering. Furthermore, the XRD patterns exhibit either no peak or a low intensity peak at $2\theta = 26^\circ$ (ascribed to the (002) diffraction from turbostratic carbon), which indicates that the carbons are amorphous or have low levels of graphitization, which is consistent with carbon deposition within the zeolite pores.^{11,20}

The porosity of the carbons was probed using nitrogen sorption. As shown in Figure 3, the carbons exhibit type I isotherms with significant adsorption below relative pressure (P/P_0) = 0.1, due to capillary filling of micropores. The isotherms are largely similar and confirm that the carbons are predominantly microporous, which is consistent with the presence of micropore channels arising from the zeolite-like structural ordering. Given the importance attributed to a potential relationship between pore size and hydrogen storage capacity, it was necessary to ascertain that the carbons had similar pore size and pore size distribution. The pore size distribution (PSD) was determined via a NLDFT model using nitrogen adsorption data. Overall, the pore size distribution of all the samples is in

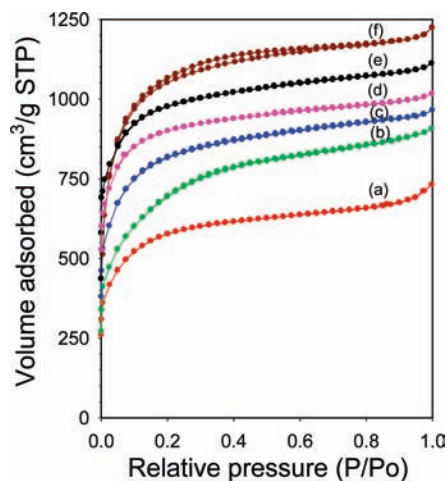


Figure 3. Nitrogen sorption isotherms of zeolite-templated carbons: (a) CY700ET, (b) CX700ET, (c) CXFAET, (d) CM800AN, (e) CM750AN, (f) CMFAET. For clarity, the isotherm for sample CM800AN is offset by 100 along the y-axis.

the same range (Supporting Information, Figure S1). The apparent magnitude and distribution of the pores confirms that zeolite templating generated a set of carbon materials with a highly similar pore channel system. However, we wish to remark that the actual pore size of the carbons, which appears from the PSD curves to be 10–12 Å, is overestimated. Indeed such a pore size is not consistent with the pore dimensions of between 6 and 8 Å measured directly from TEM images (Supporting Information, Figure S2). This overestimation seems to be a feature of NLDFT pore size obtained from nitrogen sorption data.²³ A recent report by Zhao and co-workers found that the NLDFT model using nitrogen sorption data overestimates the pore size of zeolite templated carbons by a similar magnitude,^{23a} such that while nitrogen sorption data indicated a pore size of about 11 Å, CO₂ adsorption at 273 K gave a more representative pore size of 6–9 Å. The formation of pores of size between 5 and 8 Å for zeolite-templated carbons is reasonable given that the thickness of the zeolite wall framework (which becomes the pores in the carbons) is about 0.6 nm.²⁴ Preliminary data using CO₂ adsorption on our zeolite-templated carbons yields a pore size of between 5 and 9 Å (Supporting Information, Figure S3). Nevertheless, despite some uncertainty about the actual pore size, it is clear from our data that there are no significant variations in the pore size or pore size distribution of the present carbons.

The surface area and pore volume of the carbon materials is summarized in Table 1. The carbon materials have high surface area in the range 1900–3700 m²/g and pore volume of between 0.99 and 1.88 cm³/g. There are no apparent correlations between the type of zeolite (EMC-2, Y, or 13X) used as template or method of carbon ingress (i.e., liquid impregnation, CVD, or both) and the textural properties. The presence or absence of nitrogen does not appear to have any significant effect on the textural properties. The micropore surface area (1500–2800 m²/g) and pore volume (0.65–1.24 cm³/g) of all the carbons is also high. The proportion of micropore surface area is high and is typically between 70 and 85% of the total surface area. It is

clear that the high level of zeolite-type pore ordering (Figure 2) favors high surface area, large pore volume, and enhanced microporosity.

The present zeolite templated carbons are largely similar with respect to zeolite-like ordering (Figure 2) and pore size (Supporting Information, Figures S1 and S3), and the main variables are the textural properties and the presence or absence of nitrogen. It is therefore possible to probe how changes in textural properties affect hydrogen uptake for the two sets of samples: N-doped and N-free. Hydrogen uptake capacity (both total and excess) of the carbons is shown in Table 1. The total hydrogen uptake is generally higher than that of other types of porous carbons²⁵ and varies between 4.1 and 6.9 wt %. (We verified our hydrogen uptake measurements by comparison with a well-known carbon that has previously been investigated by others. Under our hydrogen uptake measurement conditions, the activated carbon G212 (surface area and pore volume of 1405 m²/g and 0.7 cm³/g, respectively) had a total hydrogen uptake of 2.0 wt % at 1 bar and ca. 4 wt % at 20 bar, which closely matches that obtained by Zhao et al.,^{13a} who observed an uptake of 2.15 wt % at 1 bar.) The trend in hydrogen uptake capacity appears to be related to the textural properties of the carbon materials. To explore this relationship further, we have plotted in Figure 4 the variation of excess hydrogen uptake capacity with the total surface area or total pore volume. A linear relationship is observed in both cases. The observed relationship (Figure 4 and Supporting Information, Figure S4) is consistent with previous results.^{5–11,20,26} It is, however, noteworthy that, when considering the excess hydrogen uptake as a function of the total surface area (Figure 4A), the N-free samples appear to generally have a higher uptake per given surface area or per unit surface area compared to the N-doped samples.

Several studies have shown that pore channels within the micropore size range contribute most to hydrogen uptake and that larger pores are far less effective in storing hydrogen.^{5–11,25–29} Although the expectation is that hydrogen is physisorbed on all available surface sites, virtually all published studies have identified a link between hydrogen uptake in porous materials and microporosity.^{1,5–11,20,21,25–29} It is now generally accepted that there is an optimum pore size range for the adsorption of hydrogen and that an enclosed surface associated with micropores stores more hydrogen per given surface area than larger mesopore or macropore voids.^{27–29} Indeed, a recent experimental study of hydrogen storage on porous carbons has

(23) (a) Guan, C.; Wang, K.; Yang, C.; Zhao, X. S. *Microporous Mesoporous Mater.* **2009**, *118*, 503. (b) Guan, C.; Zhang, X.; Wang, K.; Yang, C. *Sep. Purif. Technol.* **2009**, *66*, 565.
(24) Su, F.; Zhao, X. S.; Lv, L.; Zhou, Z. C. *Carbon* **2004**, *42*, 2821.

(25) (a) Hirscher, M.; Panella, B. *J. Alloys Compd.* **2005**, *404*, 399. (b) Panella, B.; Hirscher, M.; Roth, S. *Carbon* **2005**, *43*, 2209. (c) Pang, J.; Hampsey, J. E.; Wu, Z.; Hu, Q.; Lu, Y. *Appl. Phys. Lett.* **2004**, *85*, 4887. (d) Xia, Y.; Mokaya, R. *J. Phys. Chem. C* **2007**, *111*, 10035. (e) Jorda-Beneyto, M.; Suarez-Garcia, F.; Lozano-Castello, D.; Ca-zorla-Amoros, D.; Linares-Solano, A. *Carbon* **2007**, *45*, 293. (f) Pacula, A.; Mokaya, R. *Microporous Mesoporous Mater.* **2007**, *106*, 147. (g) Terres, E.; Panella, B.; Hayashi, T.; Kim, Y. A.; Endo, M.; Dominguez, J. M.; Hirscher, M.; Terrones, H.; Terrones, M. *Chem. Phys. Lett.* **2005**, *403*, 363.
(26) Nishihara, H.; Hou, P. X.; Li, L. X.; Ito, M.; Uchiyama, M.; Kaburagi, T.; Ikura, A.; Katamura, J.; Kawarada, T.; Mizuuchi, K.; Kyotani, T. *J. Phys. Chem. C* **2009**, *113*, 3189.
(27) (a) Cabria, I.; Lopez, M. J.; Alonso, J. A. *Phys. Rev. B* **2008**, *78*, 075415. (b) Kim, B. J.; Lee, Y. S.; Park, S. J. *Int. J. Hydrogen Energy* **2008**, *33*, 2254. (c) Xia, K. S.; Gao, Q. M.; Song, S. Q.; Wu, C. D.; Jiang, J. H.; Hu, J.; Gao, L. *Int. J. Hydrogen Energy* **2008**, *33*, 116. (d) Jung, S. H.; Kim, H. K.; Yoon, J. W.; Chang, J. S. *J. Phys. Chem. B* **2006**, *110*, 9371. (e) Fang, B. Z.; Zhou, H. S.; Honma, I. *J. Phys. Chem. B* **2006**, *110*, 4875.
(28) Bhatia, S. K.; Myers, A. L. *Langmuir* **2006**, *22*, 1688.
(29) Gogotsi, Y.; Portet, C.; Osswald, S.; Simmons, J. M.; Yildirim, T.; Laudisio, G.; Fischer, J. E. *Int. J. Hydrogen Energy* **2009**, *34*, 6314.

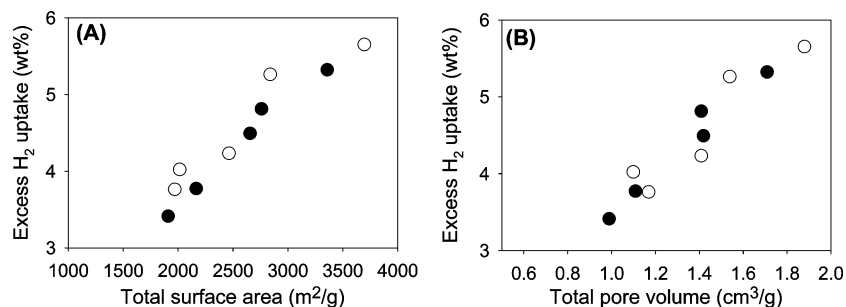


Figure 4. Excess hydrogen uptake capacity of zeolite-templated N-doped (●) and N-free (○) carbon materials as a function of (A) total surface area and (B) total pore volume.

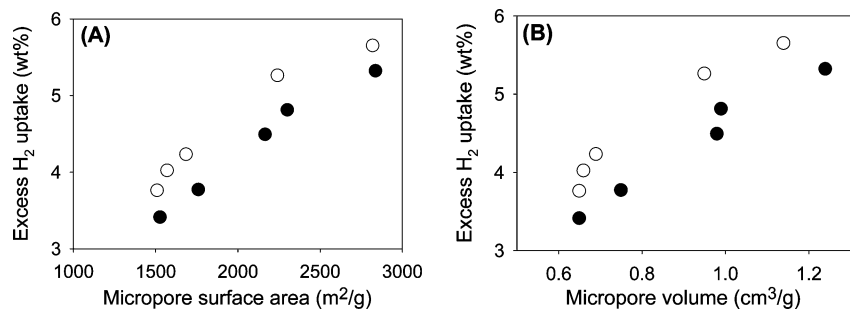


Figure 5. Excess hydrogen uptake capacity of zeolite-templated N-doped (●) and N-free (○) carbon materials as a function of (A) micropore surface area and (B) micropore volume.

concluded that pores larger than 15 Å make little contribution to hydrogen uptake at -196 °C and pressure of up to 60 bar.²⁹ Therefore, to probe the influence of nitrogen doping on hydrogen uptake, we considered the relationship between hydrogen storage capacity and the surface area/pore volume associated with micropores only. Figure 5 (and Supporting Information, Figure S5) shows a plot of excess hydrogen uptake capacity as a function of micropore surface area and micropore volume. In all cases, for similar micropore surface area or pore volume, the N-free carbons clearly have higher uptake capacity per unit micropore surface area or pore volume compared to N-doped carbons. The hydrogen storage data and textural properties are reproducible (i.e., several measurements with minimal error or variation), and therefore, the difference between the two sets of samples is significant. In particular, the hydrogen storage data was highly repeatable and virtually identical over several runs, with minimal variation (typically <1%) in uptake capacity throughout the entire pressure range (Supporting Information, Figure S6).

In evaluating the origin of the differences in hydrogen uptake depicted in Figure 5 it is important to consider the effect of any variations in the extent of mesoporosity in the carbon samples. The proportion of microporosity in the carbons is generally comparable, although some N-free samples show a slightly greater presence of mesoporosity. (The larger pores may arise from interparticle voids, incomplete filling of carbon precursor into the zeolite template during the replication process or merging of smaller pores into large ones during the carbonization and zeolite etching steps.) Recent studies indicate that mesopores contribute less to hydrogen uptake,^{26–29} thus, to a first approximation, one can plot excess hydrogen uptake as a function of micropore textural properties to investigate the effect of N-doping on the hydrogen sorption within the micropores (Figure 5). The plots of total hydrogen uptake as a function of total surface area and pore volume (Supporting Information, Figure S7) and as a function of micropore surface

area and micropore volume (Supporting Information, Figure S8) show trends that are similar to those observed for the excess hydrogen uptake (Figures 4 and 5) and that the N-doped carbons have a lower hydrogen uptake than N-free carbons of a comparable surface area. We validated our excess hydrogen uptake data by comparison with independently measured data obtained using a volumetric method with Sievert's apparatus (Supporting Information, Figure S9).

The plots in Figure 5 (and Supporting Information, Figure S8) indicate that N-doping has a negative effect on the hydrogen uptake capacity (at -196 °C and 20 bar) of the high surface area carbon materials. This experimental observation is consistent with previous theoretical studies that have suggested that the presence of nitrogen may act to reduce the overall interaction between hydrogen and the carbon surface thus influencing the overall hydrogen uptake capacity.^{15,16} The trends reported here are observed at above 10 bar pressure and relatively high hydrogen coverage (>4 wt %), which suggests that under such high hydrogen coverage conditions, the presence of nitrogen reduces either the adsorbate–adsorbent interactions or the number of available adsorption sites. In a recent theoretical study, Zhu and co-workers¹⁶ reported that nitrogen doping can decrease the overall hydrogen adsorption energy if the hydrogen is adsorbed on the nitrogen atoms and also on neighboring carbon atoms. Adsorption on carbon atoms that neighbor nitrogen is strengthened due to the electron withdrawing nature of the later, but this is more than canceled by the instability of adsorbing hydrogen atop the nitrogen.¹⁶ Experimentally, such a scenario would exist under high hydrogen coverage conditions (such as >4 wt % in the present study) where a maximum or near maximum of available sites are used for adsorption. If we assume that high adsorption energy translates to higher uptake capacity, then the experimentally observed trends in Figure 5 are consistent with the theoretical study of Zhu and co-workers.¹⁶

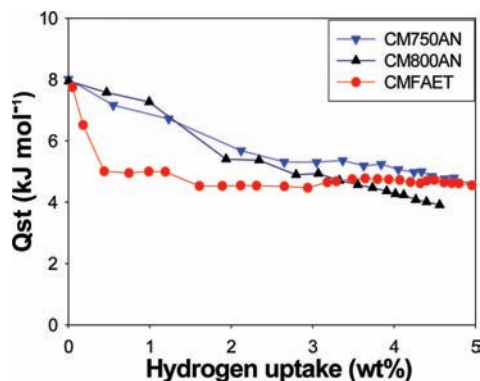


Figure 6. Isosteric heat of hydrogen adsorption (Q_{st}) as a function of the amount of hydrogen adsorbed on zeolite templated N-free (CMFAET) and N-doped (CM750AN and CM800AN) carbon materials.

However, Zhu and co-workers also observed that hydrogen adsorption energy can increase if the hydrogen is adsorbed *only* on carbon atoms neighboring the nitrogen but not on the nitrogen atom. Experimentally, such a scenario is expected to exist under low hydrogen coverage conditions. To further probe the influence of N-doping and hydrogen coverage, we compared the hydrogen adsorption energy (i.e., isosteric heat of adsorption, Q_{st}) for three samples, N-free (CMFAET) and N-doped (CM750AN and CM800AN), which were prepared from the same zeolite template. The Q_{st} values were calculated via established procedures (Supporting Information, Figure S10) using data from two different temperatures. A plot of the isosteric heat of adsorption (Q_{st}) as a function of hydrogen uptake for the three samples (Figure 6) shows that Q_{st} varies from about 8 kJ/mol at low hydrogen uptake to about 4–5 kJ/mol at high uptake (i.e., higher surface coverage).¹¹ We note that the isosteric heat of adsorption and trends observed are reliable as they were calculated using hydrogen uptake isotherms (measured at $-196\text{ }^{\circ}\text{C}$ (liquid nitrogen) and $-186\text{ }^{\circ}\text{C}$ (liquid argon)), which were highly repeatable (Supporting Information, Figure S6). The error in the Q_{st} values is very small, estimated at $\pm 1\%$. Interestingly, the data in Figure 6 shows, that at low uptake (i.e., low hydrogen coverage), Q_{st} for the N-doped carbons is higher than that of the N-free sample. However, Q_{st} for the N-doped samples gradually decreases at higher coverage, while Q_{st} for the N-free sample remains unchanged above coverage of 0.5 wt %. The overall effect is that, at higher coverage, Q_{st} for the N-doped samples drops below that of the N-free sample. This trend is in agreement with previous theoretical predictions;¹⁶ at low coverage, Q_{st} for N-doped carbons is higher (cf with N-free carbon) due to adsorption of hydrogen on favored neighboring carbons only, while at high coverage Q_{st} is lower (cf with N-free carbon) because of adsorption on both the nitrogen and the neighboring carbon atoms. We then compared the hydrogen uptake profiles of N-free (CMFAET) and N-doped (CM750AN) carbons that have comparable textural properties (Table 1). The hydrogen uptake profiles (Supporting Information, Figure S11) of the two samples appear similar at low pressure (<3 bar) but diverge at higher pressure with the N-free sample exhibiting greater hydrogen uptake (Table 1). If lowering Q_{st} is accompanied by reduced uptake, then the expected consequence of the lower Q_{st} for N-doped carbons at high coverage (e.g., at 20 bar) is clearly demonstrated in Table 1 and Figure 5 (and Supporting Information, Figures S8 and S11).

Conversely, the N-doped carbon should have higher hydrogen uptake at low pressure. Indeed, a closer analysis of the hydrogen uptake profiles for total and excess adsorption (Supporting Information, Figure S12) reveals this to be the case. The N-doped carbon (CM750AN) has slightly higher hydrogen uptake at low pressure, which then dips below that of the N-free sample (CMFAET) at higher pressure. A similar trend is observed for excess adsorption data obtained via the volumetric (Sievert's) method as shown in Supporting Information, Figure S13. Our experimental data therefore reveals good consistency with previous theoretical predictions.^{15,16}

In a previous study^{20a} we reported that carbons prepared from acetonitrile generally had higher uptake compared to those derived from ethylene. However, in that study, the porosity of the carbons was not carefully controlled as for the present samples and therefore the overriding factor in controlling the hydrogen uptake was the textural properties.^{20a} The effect of the carbon source was ascribed to ethylene being easily graphitized, while nitrogen groups (for acetonitrile derived carbons) hinder graphitization to generate carbons with higher textural properties compared to ethylene-derived carbons.^{20a} Due to greater graphitization, ethylene-derived carbons had lower surface area and low hydrogen uptake capacity, while acetonitrile-derived carbons had lower levels of graphitization, high surface area, and higher uptake capacity.³⁰ In contrast, for the present study, careful control of porosity and level of graphitisation allows the effect of N-doping to be assessed without interference from the other key factors.

Conclusions

Zeolite-templating has been used to generate a suite of carbons with similar pore size but which are either N-doped or N-free, in an attempt to demonstrate the effect of N-doping on hydrogen storage capacity. For N-doped carbons prepared using acetonitrile as carbon precursor the nitrogen content was kept within a narrow range of between 4.7 and 7.7 wt %. Bulk elemental analysis and XPS data indicated that the nitrogen was uniformly distributed. The carbon materials, irrespective of whether they were doped or not, exhibited high surface area (1900–3700 m²/g) and pore volume (0.99 and 1.88 cm³/g) and possessed a micropore surface area of 1500–2800 m²/g and a micropore volume of 0.65–1.24 cm³/g. The total hydrogen uptake varied between 4.1 and 6.9 wt %. Our findings suggest that the effect of N-doping on hydrogen uptake is only fully apparent when related to the surface area and pore volume associated with micropores rather than total porosity. By considering the hydrogen uptake and isosteric heat of hydrogen adsorption on N-free or N-doped carbons, our evidence suggests that N-doping can be beneficial at lower coverage (low hydrogen uptake) but is detrimental at higher coverage (higher hydrogen uptake). The findings represent the first attempt at experimental confirmation of previous theoretical predictions on the effect of N-doping on hydrogen uptake of carbon. The fact that the effect of N-doping is only apparent when considering hydrogen uptake as a function of microporosity (rather than total porosity) provides further evidence that pores larger than the micropore size range have a lesser role in hydrogen storage. Our findings add new insights that are useful for the development of carbon materials with enhanced hydrogen storage capacity.

(30) Kang, K. Y.; Lee, B. I.; Lee, J. S. *Carbon* **2009**, *47*, 1171.

Acknowledgment. We are grateful to Dr. Anne Dailly (General Motors, Warren, Michigan) for some of the hydrogen uptake measurements.

Supporting Information Available: An additional 13 figures; pore size distribution curves and TEM images, plots of total and excess hydrogen uptake as a function of textural properties (total or micropore surface area and pore volume),

hydrogen sorption isotherms showing repeatability of uptake measurements, hydrogen storage data used for the calculation of heats of adsorption, and hydrogen uptake profiles for samples CM750AN and CMFAET. This material is available free of charge via the Internet at <http://pubs.acs.org>.

JA9054838